

# **Influence of Substrate Initial Temperature on Adhesion Strength of Ice on Aluminum Alloy**

Tingkun Chen<sup>a</sup>, Qian Cong<sup>a,b</sup>, Chengbin Sun<sup>a</sup>, Jingfu Jin<sup>a\*</sup>, Kwang-Leong  
Choy<sup>c</sup>

<sup>a</sup> Key Laboratory of Bionic Engineering, Ministry of Education, Jilin University, Changchun  
130022, P.R.China.

<sup>b</sup> State Key Laboratory of Automotive Simulation and Control, Jilin University, Changchun  
130022, P.R.China.

<sup>c</sup> Institute for Materials Discovery, University College London, London WC1E 7JE, United  
Kingdom.

## **Abstract**

The present work investigates the influence of the initial temperature of a substrate on the ice adhesion strength by analyzing the freezing characteristics of water droplets adhered to the substrate. The ice adhesion strength on 6061 aluminum alloy was measured using a dedicated strength testing apparatus, and the freezing process of water droplets at different initial temperatures of the alloy surface was examined with a microscope. The results of the experiments show that the ice adhesion strength on the aluminum alloy surface at ambient temperature was twice as large as that measured on a colder surface (e.g., -5 °C). Combining the experimental results with the microscopic observation of the freezing process revealed that at high initial surface temperature (i.e. equal to 18 °C), the water droplets thoroughly spread on the aluminum alloy surface at high temperature, formed a larger contact area. In addition, the initial surface

---

\*Corresponding author: Jingfu Jin

Corresponding author at: 5988 Renmin Street, Changchun, 130025, P. R. China.

E-mail: [jinjingfu@jlu.edu.cn](mailto:jinjingfu@jlu.edu.cn)

Fax number: +86-431-85095575-888

23 temperature would influence the type of crystallization. Moreover, the advantages and  
24 disadvantages of thermal de-icing approaches, widely used in engineering (especially in  
25 the high-speed rail and aerospace fields), were discussed.

26 **Keywords:** Thermal de-icing; Ice adhesion strength; Initial surface temperature;  
27 Aluminum alloy; Contact interface

28

## 29 **1. Introduction**

30

31 In cold-climate regions, the inevitable accumulation of ice or wet snow on exposed  
32 surfaces severely affects many industrial activities and causes potential hazards in  
33 aircrafts, wind turbines, power lines, highways, and offshore platforms ([Gohardani et al,](#)  
34 [2013](#); [He et al., 2017](#); [Ryerson, 2011](#); [Zhu et al, 2016](#)). These issues may cause serious  
35 socioeconomic problems, and many countries have been affected by ice accumulation:  
36 for example, the collapse of power transmission lines in China owing to ice  
37 accumulation caused huge economic losses ([Ruan et al., 2016](#)). In order to ensure safe  
38 operation and efficient performance, accreted ice on a surface is usually removed by  
39 active methods, which include mechanical scraping, heating de-icing and chemical  
40 agents. However, the active methods suffer from various shortcomings, such as high  
41 costs, huge energy consumption, pollution, etc. ([Yue et al., 2016](#)).

42 In recent years, novel passive methods, in which the wettability of a surface is  
43 modified in order to improve its anti-icing ability, reduce the adhesion of water, prevent  
44 ice formation on solid surfaces, or decrease the ice adhesion strength. A particular type  
45 of passive method involves superhydrophobic surfaces (SHS), which are regarded as a  
46 promising anti-icing solution. However, several studies have highlighted the limitations

47 of SHS, such as the poor durability of their anti-icing effect (e.g., [Farhadi et al., 2011](#);  
48 [Kulinich et al., 2015](#); [Varanasi et al., 2010](#)). [Kulinich et al. \(2011a, 2011b; 2015\)](#) found  
49 that the wettability and the anti-icing ability of SHS changed during repeated  
50 icing/de-icing cycles, owing to the deterioration of the microstructure.

51 Therefore, active methods are still widely used in practical applications to remove  
52 ice accumulated on solid surfaces, especially in the high-speed rail and aviation fields,  
53 where thermal de-icing is the method of choice to melt accreted ice.

54 The fundamental mechanism of freezing of suspended or free droplets has been the  
55 subject of extensive research over the past few decades. Various efforts have been made  
56 to develop theoretical or mathematical models of droplet freezing and to validate them  
57 experimentally (e.g. [Chaudhary et al., 2014](#); [Fumoto et al., 2012](#)). [McDonald et al.](#)  
58 [\(2017\)](#) studied the crystallization of a droplet on super-cooled hydrophobic surfaces and  
59 measured the ice adhesion strength, which was essential for understanding the influence  
60 of the surface characteristics on the freezing process and developing a method to  
61 measure the ice adhesion strength on SHS.

62 In the cold regions of China, water or snow near the rails frequently attaches to the  
63 train chassis during high-speed rail operation and freezes into ice with serious  
64 consequence for the safety, comfort, and service life of the key components. In order to  
65 ensure safe operation, along with optimal performance and speed, the accreted ice on  
66 the chassis is usually removed using thermal methods. However, owing to the large  
67 temperature difference between the chassis surface and its surroundings, after removing  
68 the accreted ice by thermal methods, the melted ice may be frozen again. Furthermore,

69 it is the timing of de-icing that is critical to the thermal de-icing method.

70 Taking into account the large temperature difference after adopting thermal  
71 de-icing methods, the objective of the present work is to investigate the influence of the  
72 initial surface temperature on the ice adhesion strength on aluminum alloy. The present  
73 paper analyzes the mechanism depending on the freezing process of water droplets on  
74 solid surface at different temperatures. In addition, the influence of the initial surface  
75 temperature on the energy needed for the application of the thermal de-icing method is  
76 discussed. The results of this study provide an improved reference for the  
77 implementation of conventional thermal approaches in de-icing technologies.

78

## 79 **2. Test conditions**

80

81 The ice adhesion strength was measured under different freezing conditions, and  
82 the adhesion strength values were then used to evaluate the influence of the initial  
83 surface temperatures on the stability of the accreted ice on the sample surface. The  
84 constantly changing morphology of water droplets or ice on the aluminum alloy during  
85 the freezing process was examined with a microscope.

86

### 87 *2.1. Materials*

88

89 Aluminum alloy widely used in the aerospace industry and other engineering fields  
90 ([Ruan et al., 2016](#); [Zuo et al., 2015](#)). Therefore, in this work, 6061 aluminum alloy (40  
91  $\times 40 \times 2$  mm<sup>3</sup> in size) purchased from the Fushun Aluminum Co., Ltd., Liaoning (China)  
92 as the sample material. Ten microliters of water was dropped onto the sample surface  
93 using a micro pipette.

94

## 95 2.2. *Temperature*

96

97 Generally, ice formation takes place at low temperatures, ranging from -6 to -20 °C.

98 This same range was also selected in many previous studies (e.g. [Kermani et al., 2007](#)).

99 As the average winter temperature in China is below -20 °C, the final surface  
100 temperatures in the present study were respectively set to -5, -10, and -15 °C, which  
101 were considered as representative warm, medium, and cold environments.

102 The environmental conditions of the experiments were controlled using a climate  
103 chamber, in which the ambient temperature and humidity were maintained at  
104 approximately 18 °C, and 50%, respectively.

105

## 106 2.3. *Experimental apparatuses*

107

108 The ice adhesion strength was measured using a purposely-built apparatus to  
109 evaluate the effect of the initial surface temperature on the contact stability of ice. The  
110 freezing process of water droplets at different surface temperatures was recorded using a  
111 microscopic observation device.

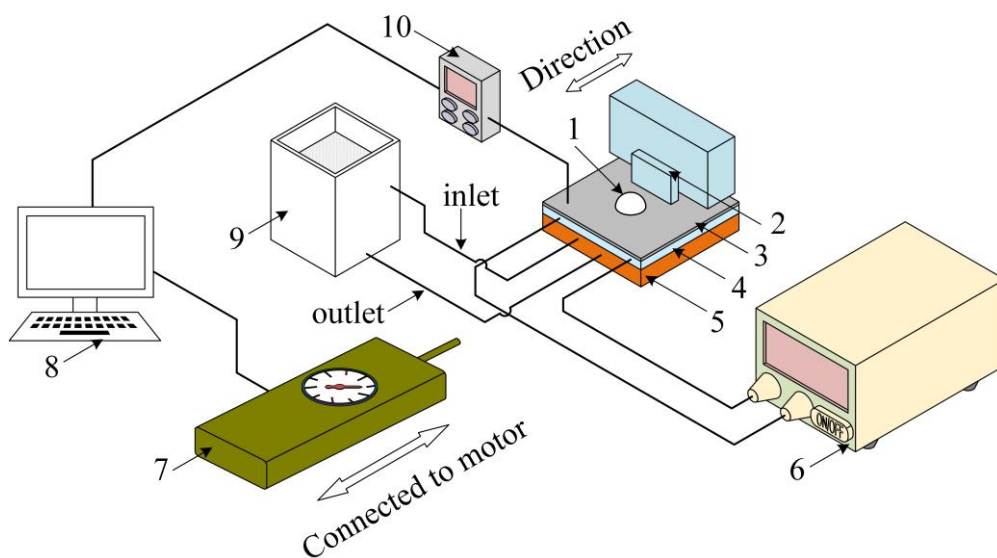
112

### 113 2.3.1 *Ice adhesion strength testing device*

114

115 The measurement method of the adhesion strength referred the [ASTM D3528](#)  
116 [\(2002\) standard](#), and the purposely built apparatus to measure the ice adhesion strength  
117 was assembled and the measured procedures was detailed according to the [ASTM](#)  
118 [D3528 \(2002\) standard](#) and the study by [Zou et al. \(2007\)](#). As shown in Fig. 1, the key  
119 components of the apparatus were freezing unit, water-cooling unit, force-measuring

120 unit, along with a push-pull mechanism. The cooling unit contained a semiconductor  
121 cooling device to refrigerate the surface, whereas the force-measuring unit included a  
122 scraper mounted on a sliding table and a draft gauge. During the testing process, the  
123 scraper pushed the ice until it was completely peeled off and the maximum peeling  
124 force was recorded by the draft gauge. The measurement precision of the draft gauge is  
125 0.01 N.

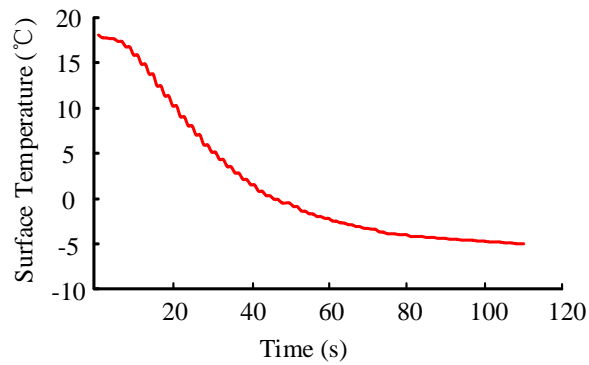


126  
127 1. Droplet (Ice); 2. Scraper; 3. Aluminum alloy; 4. Semiconductor; 5. Refrigeration  
128 stage; 6. DC power; 7. Draft gauge (connected to the motor); 8. PC; 9. Water-cooled  
129 pool; 10. Temperature Sensor.

130 Fig. 1. Schematic illustration of tangential ice adhesion strength testing device.

131

132 Since this work is focused on the influence of the temperature on the ice adhesion  
133 strength, the subsequent tests were conducted only after the surface temperature of the  
134 sample had returned to a value close to ambient temperature ( $\sim 18\text{ }^{\circ}\text{C}$ ). The temperature  
135 was measured by a K-type thermocouple located on the surface. A typical cooling curve  
136 from ambient temperature to a surface temperature of  $-5\text{ }^{\circ}\text{C}$ , is shown in Fig. 2.



137

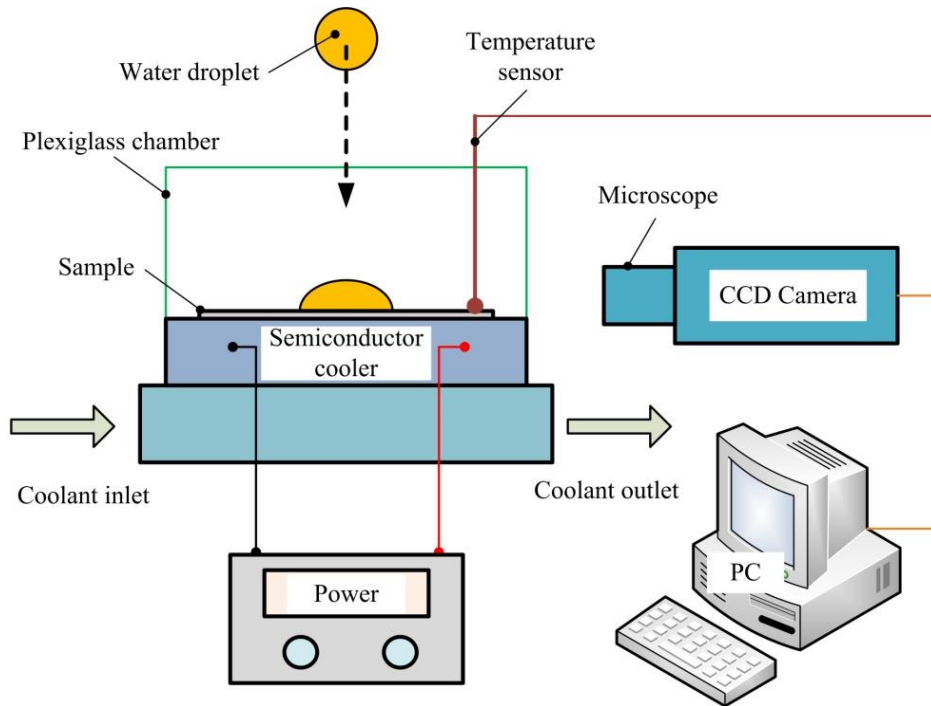
138 Fig.2. Cooling curve of a sample, showing temperatures measured at the sample  
139 surface.

140

### 141 2.3.2 Freezing process observation device

142

143 The apparatus used to monitor the freezing process, shown in Fig. 3, consisted of a  
144 microscope, an image collection system, and a cooling station with a temperature  
145 controller. The cooling station could directly refrigerate the aluminum surface. The  
146 microscope, equipped with a charge-coupled device (CCD) camera, was used to  
147 dynamically inspect the droplet morphology and the freezing process. The multichannel  
148 temperature recorder could simultaneously record the ambient, sample surface and  
149 droplet temperatures. In order to analyze the relationship between temperature and  
150 surface morphology of ice, multiple cameras were employed to synchronously monitor  
151 different parameters during the freezing process.



152

153 Fig. 3. Microscopic device and experimental set up for monitoring the freezing process

154

155 *2.4. Experimental conditions*

156

157 *2.4.1 Adhesion strength tests*

158

159 The temperature at which the water droplet made contact with the sample surface  
 160 was defined as the initial surface temperature of the aluminum alloy substrate. Two  
 161 different experimental conditions were considered, labeled Experiment 1 and  
 162 Experiment 2 in the following.

163 In the case of Experiment 1, the water droplet was placed on the aluminum alloy  
 164 substrate before cooling, i.e., the initial surface temperature was close to the ambient  
 165 temperature (18 °C). Then, the substrate and the water droplet were cooled down to the  
 166 predetermined temperature and maintained at that temperature for 3 min. Finally, the ice  
 167 adhesion strength was measured using the purposely-built device as shown in Fig. 1.  
 168 Three final temperatures (-5, -10, and -15 °C) were considered in the Experiment 1.



169 In Experiment 2, the aluminum alloy substrate was first cooled down to a specific  
170 initial surface temperature (i.e., -5, -10, or -15 °C), and the droplet was placed on the  
171 sample for 3min to cool. Then, the ice adhesion strength was measured by the device  
172 described above. As the temperature of substrate only showed a very small variation  
173 when the droplet was set in contact with the surface, this effect could be neglected.  
174 Hence, we considered the final temperature of the substrate was equal to its initial  
175 temperature.

176 In order to reduce experimental errors and random errors, each experiment was  
177 repeated at least 10 times. After each test, the residual ice on the sample surface was  
178 removed in an acetone ultrasonic bath for 5min and in a deionized water ultrasonic bath  
179 for another 5min. The samples were then dried in an oven at 60 °C.

180

#### 181 *2.4.2 Droplet freezing process*

182

183 The microscopic observation of the freezing process aimed to understand the  
184 relationship between the initial surface temperature of the substrate and the freezing  
185 characteristics, based on the observed morphological variations and the measured ice  
186 adhesion strength. For this purpose, we recorded the morphology of water droplets  
187 located on the solid surface during the freezing process, under different freezing  
188 conditions.

189

### 190 **3. Results**

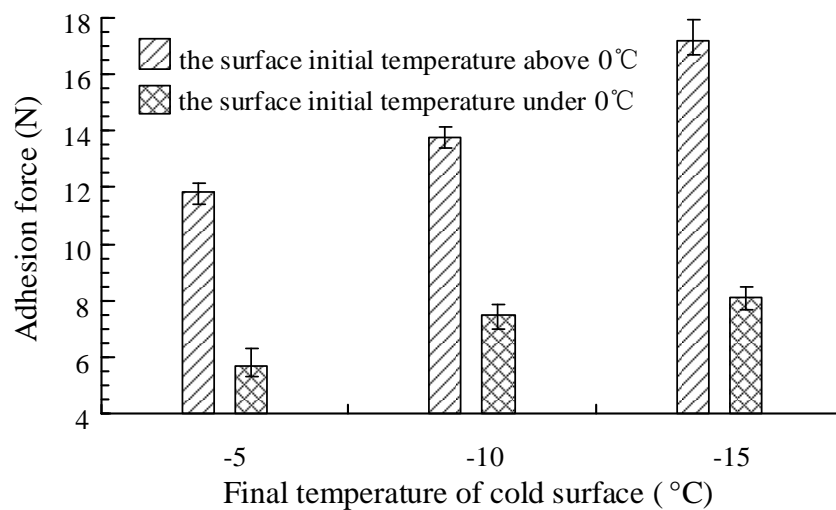
191

#### 192 *3.1. Ice adhesion strength*

193

194 The ice adhesion strengths of frozen water droplets at different initial temperatures  
 195 of the surface are summarized in Fig. 4. The results indicate that the adhesion strength  
 196 increased with decreasing final temperature, and with an approximately linear  
 197 dependence. The ice adhesion strength measured in Experiment 1 was about twice that  
 198 obtained in Experiment 2.

199 When the final temperature of the substrate surface was reduced from -5 to -15 °C,  
 200 the rate of increase in adhesion strength for Experiment 2 was lower than for  
 201 Experiment 1. In particular, when the final temperature ranged from -10 to -15 °C, the  
 202 peeling strength measured in Experiment 2 was significantly smaller than that obtained  
 203 in Experiment 1.



204

205 Fig.4. Measured ice adhesion strength for different surface temperatures.

206

### 207 3.2. Droplet morphology

208

209 In order to gain a better understanding of the relationship between initial surface  
 210 temperature and ice adhesion strength, the freezing process of a single water droplet (10  
 211 μl) with a final temperature of -10 °C was inspected under two different cooling

212 conditions. The area of the contact interface was measured immediately after placing  
 213 the droplet onto the aluminum surface. The initial height of the water droplet on the  
 214 aluminum alloy and width of the contact interface zone were approximately 1.57 and  
 215 3.05 mm, respectively.

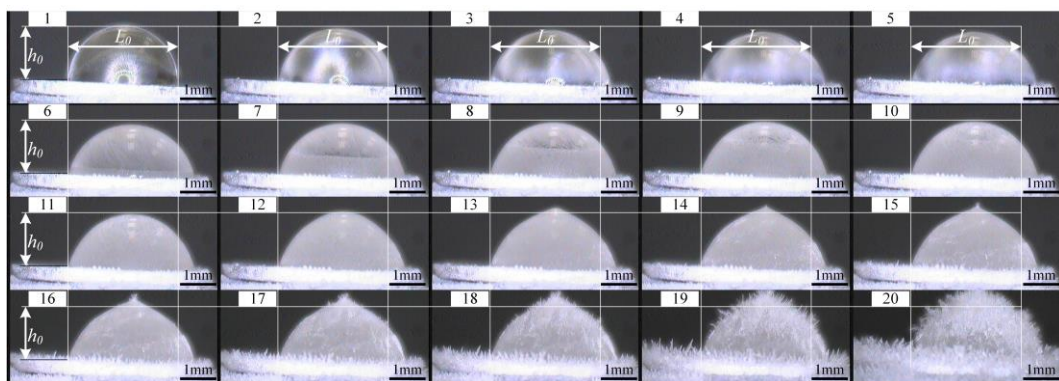
216

217 *3.2.1 Experiment 1*

218

219 Fig. 5 illustrates the time evolution of the appearance freezing water droplet under  
 220 the ‘Experiment 1’ conditions. As shown in figure, the freezing process can be divided  
 221 into five stages: initially, water droplet got muddy and lost its transparency; at the same  
 222 time, the contact area between the droplet and the surface of aluminum alloy increased;  
 223 then, phase change and solidification processes started, followed by freezing of the  
 224 water droplet and changes in the surface morphology of ice (in agreement with  
 225 [Arianpour et al., 2013](#) and [McDonald et al., 2017](#)); finally, frost was formed on the  
 226 outer-shell of ice (images 16 to 20 in Fig. 5).

227



228 Fig.5. Images showing the time evolution of a water droplet freezing on the substrate  
 229 under Experiment 1 conditions.  $h_0$ ,  $L_0$ , were the initial height of the water droplet and  
 230 width of contact interface between droplet or ice and aluminum alloy, respectively.

231

232 After being placed on the sample surface, the continuous cooling of the droplet  
233 resulted in its transparency decreasing from top to the bottom, with a simultaneous  
234 increase in height owing to the expanding contact area. Going from image 1 to 5 of Fig.  
235 5, the maximum diameter of the water droplet on the 6061 aluminum alloy increased to  
236 3.47 mm, i.e., 1.14 times larger than that of the initial state, while the contact area  
237 increased by 1.30 times (image 5 of Fig. 5).

238 As the freezing progressed, the water droplet fully changed into an opaque state  
239 and a solid-liquid interface emerged, dividing the water-ice mixture in a darker and a  
240 brighter regions. At the same time, the height of the solid-liquid mixture increased and  
241 approached the initial height of the droplet (images 6-11 in Fig. 5). Comparing images  
242 11 and 5 in Fig. 5 reveals, no obvious changes in the contact area; however, the height  
243 of the water droplet changed and increased. Therefore, it can be concluded that a  
244 volume expansion occurred as the solid-liquid interface moved from the bottom to the  
245 top of the water droplet.

246 Owing to the constraint and propelling effect of the frozen liquid, the remaining  
247 water had to move upwards and frozen into a peak. A clear increase in the height of the  
248 frozen droplet could be observed remarkably going from image 12 to image 15 of Fig. 5,  
249 leading to a peach-like appearance. However, no changes in the contact interface area  
250 were observed.

251 Images 15-20 of Fig. 5 illustrate the frost formation on the outer shell of the frozen  
252 droplet. Frosting first appeared at the top of the “peach” shape and then gradually  
253 covered it. As the cooling continued, the thickness of the frost layer began to increase.

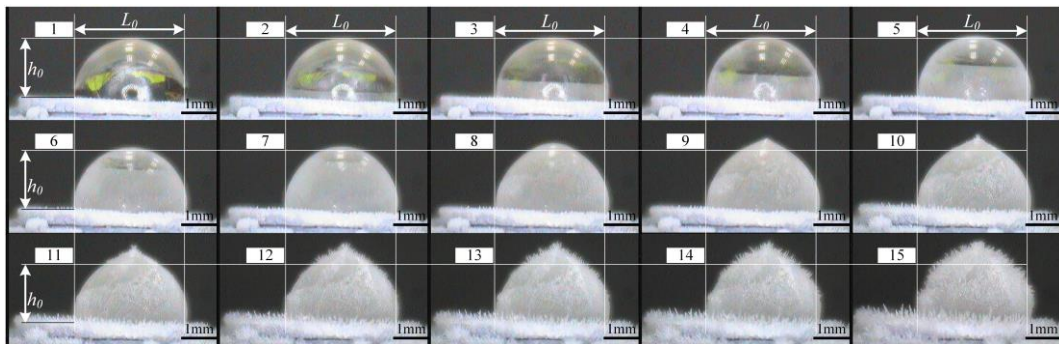
254

### 255 3.2.2 Experiment 2

256

257 The images in Fig. 6 illustrate the time evolution of a water droplet freezing on the  
258 Al-alloy substrate under the conditions of Experiment 2. In this case, the freezing  
259 process can be divided into four stages: the formation and displacement of the  
260 solid-liquid interface, shape change, freezing and frost formation.

261



262 Fig.6. Images showing the time evolution of a water droplet freezing on the Al-alloy  
263 substrate under the conditions of Experiment 2.

264

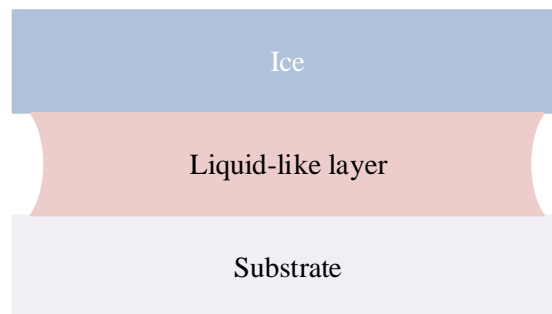
265 In the initial stage, the solid-liquid interface emerged shortly after placing the  
266 water droplet was placed on the 6061 aluminum alloy surface, and moved rapidly from  
267 the bottom to the top of the droplet. During this process (images 1-7 of Fig. 6), no  
268 significant changes in contact area were observed, although the shape of the droplet did  
269 change. As the cooling continued, the height of the water droplet showed a marked  
270 increase and the liquid droplet froze, forming the solid ice (images 8-10 of Fig. 6). At  
271 the same time, the hemisphere shape of the droplet assumed a peculiar peach-like  
272 appearance. Frost started to form on the tip of the frozen droplet and gradually covered  
273 its entire outer-surface (images 11-15 of Fig. 6).

274

#### 275 4. Discussion

276

277 In order to gain a better understanding of the ice adhesion, we applied the  
278 liquid-like layer (LLL) theory proposed by [Michael Faraday \(1859\)](#). The LLL separates  
279 the ice layer from the substrate, as shown in Fig. 7. This assumption has been validated  
280 by several studies ([Engemann et al., 2004](#); [Guerin et al., 2016](#); [He et al., 2017](#); [Mezger  
281 et al., 2008](#); [Rosenberg, 2005](#)).



282

283 Fig. 7 Adhesion model based on the liquid layer theory.

284

284 We infer that different initial surface temperatures would cause a change in the  
285 properties of the LLL, which are influenced by the spreading ability of the droplet and  
286 the structural stability of ice.

287

#### 288 4.1. Influence of contact area on ice adhesion strength

289

290 The comparison of the experimental conditions corresponding to Experiment 1 and  
291 Experiment 2 indicated that the aluminum alloy substrate in Experiment 1 had a higher  
292 surface energy, which resulted in a stronger interaction between surface and droplet.  
293 Therefore, the droplets spread more rapidly and resulted in a larger contact area in the  
294 case of Experiment 1. The LLL between ice and substrate would not freeze immediately,

295 enabling the water droplets to spread and extend the contact area (images 1-5 of Fig. 5).  
296 The capillary forces created by the LLL increased, entailing a higher energetic cost for  
297 the accreted ice on the substrate to be removed from the surface. On the other hand, the  
298 lower surface energy of the substrate in Experiment 2 resulted in a weaker interaction  
299 with droplets, and the frozen LLL would limit their spread on the Al-alloy surface  
300 (images 1-7 of Fig. 6).

301

#### 302 *4.2. Influence of contact stability on ice adhesion strength*

303

304 In Experiment 1, the substrate and the droplets were simultaneously refrigerated,  
305 and the water droplets were in a supercooled state. Supercooled water does not freeze  
306 until the process is initiated by some external factors. Following the continuous  
307 reduction in the initial temperature of the surface, and the molecular energy of the water  
308 droplet would continuously decrease until the predetermined temperature was reached.  
309 Under the conditions of Experiment 1, the droplet spent a long time in the supercooled  
310 state. If the duration of the freezing process of the droplet on the cold surface was  
311 sufficiently long, the temperature difference between the two systems would change  
312 slowly, leading to a steady and prolonged the heat exchange, and resulting in a more  
313 effective contact between the droplet and the surface; therefore, an enhanced stability of  
314 the frozen interface would be achieved under these conditions.

315 On the other hand in Experiment 2, the aluminum alloy substrate was cooled first.  
316 In this case, when a water droplet was rested on the cold surface, the latter would have a  
317 restraining effect on the liquid layer. In addition, the small size of the water droplet led

318 to low heat absorption, resulting in a shorter freezing time.

319 Furthermore, the temperature of the sample surface was much lower than the  
320 ambient temperature. After being dropped onto the surface, the droplet was rapidly  
321 cooled by the substrate surface, and its energy decreased. Due to the shorter freezing  
322 time, the temperature of the droplet changed rapidly, with a consequently shorter heat  
323 exchange time. Therefore, the water droplet froze before making sufficient contact with  
324 the Al alloy substrate. This rapid freezing process caused crack initiation, which in turn  
325 resulted in instability and deterioration of the contact interface between ice and  
326 substrate.

327

## 328 **5. Conclusion**

329

330 The ice adhesion strength of the water droplet on a cold substrate was measured by  
331 a purposely-built apparatus conform to the ASTM standard. We inspected the  
332 morphological changes of the droplet during the freezing process, and analyzed the  
333 influence of the initial surface temperature on the freezing characteristics of the  
334 droplets.

335 The analysis showed that the ice adhesion strength measured under the conditions  
336 of Experiment 1 was approximately twice that obtained in Experiment 2. This indicates  
337 that the ice adhesion strength decreased for a lower initial surface temperature under  
338 otherwise identical conditions, including final surface temperature and other test  
339 parameters, and forms a more stable contact between ice and the substrate in  
340 Experiment 1. Hence, it will need more energy or cost to remove the accumulated ice on



341 materials surface. Based on the experimental results and the inspection of the freezing  
342 process, the influence of the initial surface temperature on the ice adhesion strength can  
343 be attributed to two main causes: (1) the two test conditions involved a different effect  
344 of the cold surface on the water droplet during its freezing process, also with a different  
345 contact area between ice and substrate; (2) the large initial surface temperature  
346 difference of between substrate and droplet markedly affected the freezing time. In  
347 particular, a short freezing time resulted in unstable heat exchange between substrate  
348 and droplet, which in turn produced structural defects at the contact interface.

349 In conclusion, the experimental methods adopted in this paper simulate the  
350 influence of surface initial temperature on the freezing characteristics before and after  
351 using thermal de-icing. The results of the experiments demonstrate that surface initial  
352 temperature has a great influence on ice adhesion strength. The present paper provides  
353 an experimental basis for optimizing and reducing the cost of thermal de-icing processes,  
354 which will be highly useful within the rapid development of high-speed rail transport.

355

### 356 **Acknowledgements**

357

358 This work was supported by the international exchanges scheme between the  
359 Royal Society and the NSFC [Grant No. 51711530236].

360

### 361 **References**

362

363 ASTM D3528-96, 2002. [Standard test method for strength properties of double](#)  
364 [lap-shear adhesive joints by tension loading.](#)

365 Arianpour, F., Farzaneh, M., Kulinich, S.A., 2013. [Hydrophobic and ice-retarding](#)  
366 [properties of doped silicone rubber coatings. Appl. Surf. Sci. 265, 546-552.](#)

367 Chaudhary, G., Li, R., 2014. [Freezing of water droplets on solid surfaces: An](#)  
368 [experimental and numerical study. Exp. Therm. Fluid Sci. 57, 86-93.](#)

369 Engemann, S., Reichert, H., Dosch, H., et al, 2004. [Interfacial Melting of Ice in Contact](#)  
370 [with SiO<sub>2</sub>. Phys. Rev. Lett. 92\(20\), No. 205701.](#)

371 Farhadi, S., Farzaneh, M., Kulinich, S.A., 2011. [Anti-icing performance of](#)  
372 [superhydrophobic surfaces. Appl. Surf. Sci. 257\(14\), 6264-6269.](#)

373 Fumoto, K., Kawanami, T., 2012. [Study on Freezing Characteristics of Supercooled](#)  
374 [Water Droplets Impacting on Solid Surfaces. J. Adhes. Sci. Technol. 26\(4-5\),](#)  
375 [463-472.](#)

376 Guerin, F., Laforte, C., Farinas, M.I., et al., 2016. [Analytical model based on](#)  
377 [experimental data of centrifuge ice adhesion tests with different substrates. Cold](#)  
378 [Reg. Sci. Technol. 121, 93-99.](#)

379 Gohardani, O., Hammond, D.W., 2013. [Ice adhesion to pristine and eroded polymer](#)  
380 [matrix composites reinforced with carbon nanotubes for potential usage on future](#)  
381 [aircraft. Cold Reg. Sci. Technol. 96, 8-16.](#)

382 He, Z.W., Vågnes, E.T., Delabahan, C., et al, 2017. [Room Temperature Characteristics](#)  
383 [of Polymer-Based Low Ice Adhesion Surfaces. Sci. Rep. 7, No, 42181.](#)

384 Kermani, M., Farzaneh, M., Gagon, R., 2007. [Compressive strength of atmospheric ice.](#)  
385 [Cold Reg. Sci. Technol. 49\(3\), 195-205.](#)

386 Kulinich, S.A., Honda, M., Zhu, A.L., et al, 2015. [The icephobic performance of](#)

387 [alkyl-grafted aluminum surfaces. \*Soft Matter\*. 11\(5\), 856-861.](#)

388 [Kulinich, S.A., Farzaneh, M., 2011. On ice-releasing properties of rough hydrophobic](#)  
389 [coatings. \*Cold Reg. Sci. Technol.\* 65\(1\), 60-64.](#)

390 [Kulinich, S.A., Farhadi, S., Nose, K., et al., 2011. Superhydrophobic Surfaces: Are They](#)  
391 [Really Ice-Repellent?. \*Langmuir\*. 27\(1\), 25-29.](#)

392 [McDonald, B., Patel, P., Zhao, B.X., 2017. Droplet freezing and ice adhesion strength](#)  
393 [measurement on super-cooled hydrophobic surfaces. \*J. Adhes.\* 93\(5\), 375-388.](#)

394 [Michael Faraday, 1859. Note on Regelation. \*Proceedings of the Royal Society of\*](#)  
395 [London 10: 440-450.](#)

396 [Mezger, M., Schöder, S., Reichert, H., et al., 2008. Water and ice in contact with](#)  
397 [octadecyl-trichlorosilane functionalized surfaces: A high resolution x-ray](#)  
398 [reflectivity study. \*J. Chem. Phys.\* 128\(24\), No, 244705.](#)

399 [Ryerson, C.C., 2011. Ice protection of offshore platform. \*Cold Reg. Sci. Technol.\* 65\(1\),](#)  
400 [97-110.](#)

401 [Ruan, M., Wang, J.W., Liu, Q.L., et al, 2016. Superhydrophobic and Anti-Icing](#)  
402 [Properties of Sol–Gel Prepared Alumina Coatings. \*Russian J. Non-Ferr. Met.\* 57\(6\),](#)  
403 [638–645.](#)

404 [Rosenberg, R., 2005. Why is ice slippery?. \*Phys. Today\*. 58\(12\), 50-55.](#)

405 [Varanasi, K.K., Deng, T., Smith, J.D., et al., 2010. Frost formation and ice adhesion on](#)  
406 [superhydrophobic surfaces. \*Appl. Phys. Lett.\* 97 \(23\), No. 234102.](#)

407 [Yue, X.F., Liu, W.D, Wang, Y., 2016. Effects of black silicon surface structures on](#)  
408 [wetting behaviors, single water droplet icing and frosting under natural convection](#)

409            conditions. *Surf. Coat. Technol.* 307, 278-286.

410    Zou, M., Beckford, S., Wei, R., et al., 2011. [Effects of surface roughness and energy on](#)  
411            [ice adhesion strength.](#) *Appl. Surf. Sci.* 257(8), 3786-3792.

412    Zhu, Y.C., Huang, X.B, Jia, J.Y., et al, 2016. [Experimental study on the thermal](#)  
413            [conductivity for transmission line icing.](#) *Cold Reg. Sci. Technol.* 129, 96-103.

414    Zuo, Z.P., Liao, R.J, Guo, C., et al., 2015. [Fabrication and anti-icing property of](#)  
415            [coral-like superhydrophobic aluminum surface.](#) *Appl. Surf. Sci.* 331, 132-139.